Signal and Image Processing Letters
Vol. 5., No. 2, 2023, pp. 9-19
ISSN 2714-6677
https://simple.ascee.org/

Computation and analysis of highly stable and efficient non-toxic perovskite $CsSnGeI_3$ based solar cells to enhance efficiency using SCAPS-1D software

Md. Momin Hossain [a,1,*], Md. Yakub Ali Khan [a,2], Md. Abdul Halim [b,3], Nafisa Sultana Elme [a,4], Md. Shoriful Islam [d,5].

[a] Department of Electrical and Electronic Engineering, World University of Bangladesh, Uttara, Dhaka 1230, Bangladesh
[b] Electrical, Electronic and Computer Engineering, The University of Catania, Sicily, Italy
[c] Department of Computer Science and Engineering, World University of Bangladesh, Uttara, Dhaka 1230, Bangladesh
[1]hmomin89@gmail.com; [2]yakub.bimt@gmail.com; [3]halimabdul552@gmail.com; [4]nafisaelme111@gmail.com; [5]shoriful.islam23@outlook.com
* corresponding author

ARTICLE INFO

Keywords
Perovskite-based solar cell (PSC)
TiO_2 buffer
$CsSnGeI_3$ absorber
Renewable and Sustainable
SCAPS-1D

ABSTRACT

This paper examines the physical, optical, and electrical characteristics of cesium tin-germanium triiodide based single halide Perovskite absorption materials in order to provide the best photovoltaic application. In light of the diversification of the use of natural resources, perovskite solar cells are becoming more and more essential for capturing renewable energy. In this research work, a cesium tin–germanium triiodide ($CsSnGeI_3$) perovskite-based solar cell (PSC) has been reported to achieve a high-power-conversion efficiency (PCE). $CsSnGeI_3$ perovskite-based solar cell has been proposed for the Pb and toxic-free (Al/FTO/ TiO_2/$CsSnGeI_3$/Mo) structure simulated in Solar Cell Capacitance Simulator (SCAPS-1D software. At first aluminum, fluorine-doped tin oxide, Titanium dioxide, cesium tin–germanium triiodide and Molybdenum have been inserted into SCAPS and simulated using specific temperature. In this simulation, the electron transport layer (ETL) FTO, the buffer layer TiO_2, and the absorber layer $CsSnGeI_3$ were all used. Utilizing variations in thickness including absorber and buffer, defect density, operating temperature, back contact work function, series and shunt resistances, acceptor density, and donor density, the performance of the proposed photovoltaic devices was quantitatively assessed. Throughout the simulation, the absorber layer thickness was held constant at 1.6 µm, the buffer layer at 0.05 µm, and the electron transport layer at 0.5 µm. A solar cell efficiency of 24.75%, an open-circuit voltage of 0.95 volts, a short-circuit current density of 30.61 mA/cm2, and a fill factor (FF) of 85.42% have all been recorded for the $CsSnGeI_3$ absorber layer. Our ground-breaking findings unequivocally show that $CsSnGeI_3$-based PSC is a strong contender to quickly overtake other single-junction solar cell technologies as the most effective.

1. Introduction

For the development of all industries, energy is a nation's backbone. Concerns regarding the development of clean and renewable energy [1] sources solar [2], wind, mechanical vibration [3] are raised by the increasing rate of fossil fuel depletion and their negative effects on the environment. As the light-harvesting active layer in a perovskite solar cell, a substance with a perovskite structure is utilized; normally, this substance is a hybrid organic-inorganic lead or tin halide-based compound [4,5]. This promises to lower production costs and produce semiconductors of excellent quality. Perovskite solar cells (PSCs) have recently become one of these candidates [6–8]. There have been reports of great power conversion efficiency and exceptional air stability [9] in perovskite-based solar cells (PSCs) made of cesium tin-germanium triiodide ($CsSnGeI_3$). The all-inorganic lead-free $CsSnI_3$ perovskite may be a promising replacement for Pb-based light harvesting materials due to its superior photoelectric properties, including a high absorption coefficient, small exciton binding energy, high carrier mobility, etc. Currently, it is the most competitive candidate [10-13]. However, the $CsSnGeI_3$perovskite's phase instability and the self-oxidation of Sn from Sn^{2+} to Sn^{4+} hinder its future use as a solar cell [14]. Recently Min Chen et al. have reported that alloying $CsSnI_3$ with Ge (II) to form a $CsSn_{0.5}Ge_{0.5}I_3$ gives highly sTable and air tolerant perovskite solar cell [15].

A number of ETL layer materials, including ZnO: $Al, FTO, ITO, TiO_2, CdS,$ and CeO_2, have also been tested with absorber layers to increase efficiency in this area [16–23]. When FTO has been utilized as an Electron Transport Layer (ETL) to achieve maximum efficiency and is better suited for the absorber layer $CsSnGeI_3$. Maximum efficiency is what the electron transport layer seeks to achieve.

Solar cells made of $CsSnGeI_3$ have a number of benefits but also some drawbacks. Due to its wide bandgap, $CsSnGeI_3$ is a good choice for capturing solar energy in the visible to near-infrared spectrum. The constituent elements of $CsSnGeI_3$ are cesium (Cs), tin (Sn), germanium (Ge), and iodine (I), all of which are abundant and very inexpensive. In comparison to certain other perovskite compositions, $CsSnGeI_3$'s composition is composed of elements that are abundant on Earth and does not rely on rare or hazardous compounds.

The power conversion efficiencies of $CsSnGeI_3$-based solar cells have been shown to be respecTable, however they are often lower than those of lead-based perovskite solar cells. In order to improve the effectiveness and performance of $CsSnGeI_3$-based devices, additional research and development are required. Compared to some other perovskite compositions, $CsSnGeI_3$ has demonstrated greater stability, however stability issues still exist. The study of the characteristics and performance of the relatively new perovskite material $CsSnGeI_3$ is still in progress. It can be difficult to synthesize and produce $CsSnGeI_3$-based solar cells on a large scale. In order to solve the drawbacks of $CsSnGeI_3$-based solar cells and further enhance their performance, stability, and scalability, research and development efforts are still being made. Future practical uses of $CsSnGeI_3$-based solar cells may be enhanced by ongoing improvements in materials, device designs, and production methods.

To create a highly effective and sTable structure without the use of harmful materials, $CsSnGeI_3$ has been chosen for the absorber layer and TiO_2 is the buffer layer for the first time in this research work. The fact that it is a perovskite solar cell without HTL prevents this construction from becoming costly and complicated. FTO was utilized as an ETL, and this setup produced great results. The front contact and the back-contact Mo are used in the $CsSnGeI_3$-based perovskite solar cell. SCAPS-1D software has been used to analyze each observation. More investigation has been done on this perovskite solar cell in this study. The thickness of the absorber layer ($CsSnGeI_3$) has also been altered, with corresponding effects on the power conversion efficiency (PCE), open circuit voltage (VOC), short-circuit current density (JSC) and fill factor (FF). The output parameters were altered after adjusting the thickness of the absorber layer.

2. Method

At the Department of (EIS) in Belgium, a program named SCAPS-1D-short for "Solar Cell Capacitance Simulator One-dimensional"-was developed to simulate solar cells [38,39]. This device

doesn't have the same generality as the cells in used here. Fig. 1 shows the $Al/FTO/TiO_2/CsSnGeI_3/Mo$ structural characterization of the device is created and simulated using the SCAPS-1D software program. In the proposed structure TiO_2 was used as buffer layer, FTO used as ETL layer in $CsSnGeI_3$ based perovskite-based solar cell (PSC).

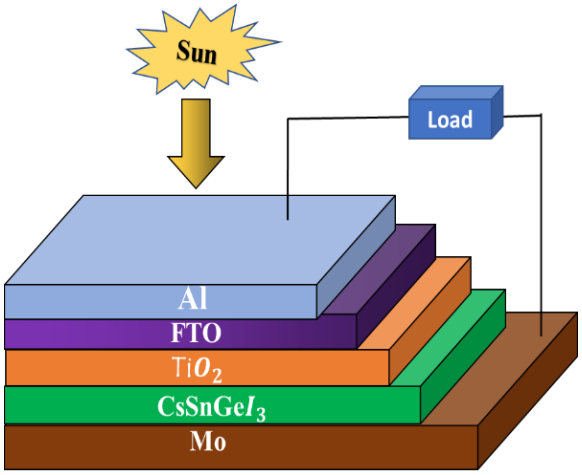

Fig. 1. Schematic diagram of the proposed CsSnGeI3 based perovskite-based solar cell (PSC) having the structure of $Al/FTO/TiO_2/CsSnGeI_3/Mo$

The simulation was performed at a temperature of 300 K under standard illumination of 1000 W/m^2, and an air mass of AM 1.5 G. As shown in the figure, the electron transport layer (ETL) FTO, the buffer layer TiO_2, and the absorber layer $CsSnGeI_3$. As a front contact and back metal, aluminum (Al) and Mo were used, respectively.

There are a few restrictions to take into account while using SCAPS 1D (Solar Cell Capacitance Simulator 1D) to simulate $CsSnGeI_3$-based solar cells. SCAPS 1D makes use of material models that are predicated on particular hypotheses and variables. These simulations might not accurately represent the special electrical and optical characteristics of $CsSnGeI_3$. For precise performance estimates, the simulation of interactions between several layers of a solar cell is essential. It can be difficult to precisely simulate the interfaces and the related interfacial effects, though. It's possible that the complexity and variety of device topologies employed in $CsSnGeI_3$-based solar cells will not be adequately captured by SCAPS 1D, which assumes a one-dimensional device structure. Time-dependent impacts and degradation mechanisms are not automatically taken into consideration by SCAPS 1D, which primarily concentrates on steady-state simulations.

Despite these drawbacks, SCAPS 1D can nevertheless offer insightful analysis and qualitative comprehension of the performance trends and device properties of solar cells based on $CsSnGeI_3$. It can be a helpful tool for preliminary device optimization and for examining how various settings affect the functioning of the device. However, to take into consideration the unique characteristics and difficulties related to $CsSnGeI_3$-based solar cells, it is crucial to test the simulation results with experimental data and take into account more sophisticated simulation methodologies or approaches.

Unique optical properties of perovskite $CsSnGeI_3$-based solar cells influence their photovoltaic performance. Effective light absorption is made possible by the fact that $CsSnGeI_3$ has a reasonably high absorption coefficient over a wide spectrum of wavelengths. Solar cells made of $CsSnGeI_3$ can absorb light in the visible to near-infrared (NIR) range, which accounts for a sizeable fraction of the solar spectrum. As a result of photon absorption, $CsSnGeI_3$ exhibits a direct bandgap, which allows electrons in the valence band to be directly promoted to the conduction band. The luminescence of $CsSnGeI_3$ emits light in the visible spectrum. Researchers can further enhance light absorption, charge generation, and charge collecting within the solar cells by making use of these optical features, resulting to improved efficiency and general performance.

Using SCAPS-1D software, a number of potential research and development directions can be investigated in order to improve the performance of non-toxic perovskite $CsSnGeI_3$-based solar cells. The material characteristics of $CsSnGeI_3$ and its alloys can be further investigated to find potential improvements. The efficiency of charge extraction, recombination, and the entire device can be

considerably increased by improving the interfaces between the various layers inside the solar cell structure. Maximizing light absorption and reducing losses in the solar cell depend on effective light management. Researchers can improve the effectiveness, stability, and general performance of non-toxic perovskite $CsSnGeI_3$-based solar cells by concentrating on these research areas, using SCAPS-1D simulations, and incorporating experimental validation, increasing the likelihood that these solar cells will find use in real-world renewable energy applications. The SCAPS 1D program was used to extract the energy band diagram for suggested $Al/FTO/TiO_2/CsSnGeI_3/Mo$ thin-film solar cell. The optical characteristics of solar cells are discussed using the energy band diagram. The arrow indicates the movement of electron and holes in Fig. 2.

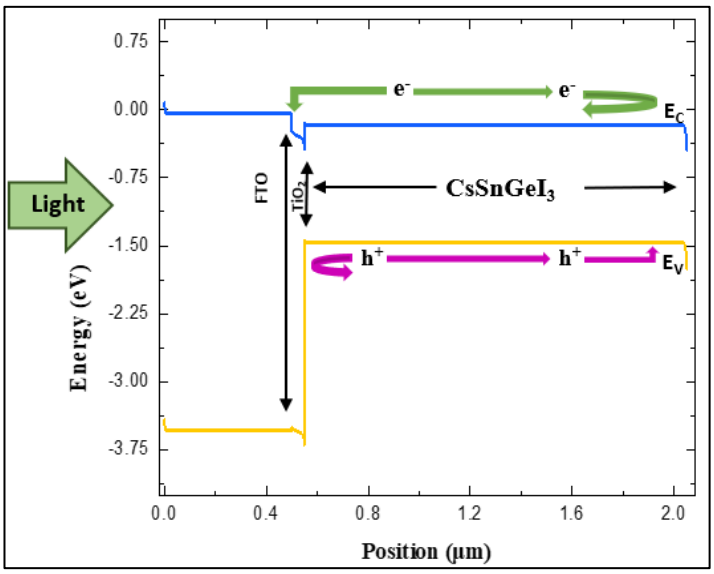

Fig. 2. Energy band diagram of $CsSnGeI_3$ based perovskite-based solar cell (PSC) Solar cell.

Table 1. Physical parameters of each layer used in the simulation $FTO, TiO_2, CsSnGeI_3$ (VB = valence band, CB = conduction band)

Parameters (unit)	FTO (ETL) [16]	TiO_2 (buffer) [19]	$CsSnGeI_3$ (absorber) [9,16]
Thickness (µm)	0.5	0.05	1.6
Bandgap (eV)	3.5	3.26	1.3
Electron affinity (eV)	4	4.2	3.9
Dielectric permittivity (relative)	9	10	28
CB effective DOS (cm^{-3})	2.2E+18	2.2E+18	3.1E+18
VB effective DOS (cm^{-3})	1.8E+19	1.8E+18	3.1E+18
Electron thermal velocity (cm/s)	1.E+7	1.E+7	1E+7
Hole thermal velocity (cm/s)	1.E+7	1.E+7	1E+7
Electron mobility (cm^2/V^{-s})	2.000E+1	2.E+1	9.740E+2
Hole mobility (cm^2/V^{-s})	1.000E+1	1E+1	2.130E+2
Donor density ND (cm^{-3})	1.E+19	1.E+17	0
Acceptor density NA (cm^{-3})	0	0	1.E+19

3. Result and Discussion

The primary goal of this thesis is to examine the effectiveness of a cesium tin-germanium triiodide in converting power ($CsSnGeI_3$) In order to construct real-time solar photovoltaic devices with the best power conversion efficiency (PCE), we will need to employ the optimized data. This in-depth investigation allowed us to measure the QE(η), PCE (η), Fill Factor (%), Open-circuit Voltage (VOC) and Short-Circuit current (JSC) in the Cs_2TiI_6 based thin film solar cell, allowing the research community to develop more efficient solar cell devices. In this paper $Al/FTO/TiO_2/CsSnGeI_3/Mo$ perovskite solar cell has been investigated and found that solar cell efficiency of 24.75%, an open-circuit voltage of 0.95 volts, a short-circuit current density of 30.61 mA/cm^2, and a fill factor (FF) of 85.42% shown in Table 2.

SCAPS 1D can nevertheless provide comprehensive analysis and qualitative knowledge of the performance patterns and device characteristics of solar cells based on $CsSnGeI_3$, despite these disadvantages. It can be a useful tool for performing preliminary device optimization as well as for analyzing how different settings affect the device's performance. Nevertheless, it is essential to compare the simulation results with practical data and take into account more advanced simulation methodologies or approaches in order to account for the specific characteristics and challenges associated with $CsSnGeI_3$-based solar cells. The results of this experiment show that the values of the VOC, JSC, FF and PCE do not significantly change for much thicker absorbing layers of $CsSnGeI_3$ after 1.6 µm because the incoming photons are completely absorbed by the absorbent material at the larger thicknesses. The rate of bulk recombination is accelerated because the electron-hole pair cannot enter the space charge area due to an increase in charge carrier diffusion length. The ideal thickness for the $CsSnGeI_3$ absorbent layer will therefore be considered to be 1.6 µm.

Table 2. Perovskite parameters for the $CsSnGeI_3$ based solar cell

Device Structure	Open circuit Voltage VOC(V)	Current Density JSC (mA/cm2)	Fill Factor FF (%)	Efficiency η (%)
$Al/FTO/TiO_2/CsSnGeI_3/Mo$	0.95	30.61	85.42	24.75

3.1. J-V Characteristics of CsSnGeI$_3$ Based PSC

The developed solar cell's J-V characteristics and various absorber thicknesses are shown in Fig. 3 The thickness of the absorber layer ranged from 0.1 µm to 2.5 µm, respectively. The J-V curve in Fig. 3 illustrates how current and voltage increase as absorber thickness increases. The addition of the electron-hole pair during the thickening of the absorber has the effect of increasing current and voltage.

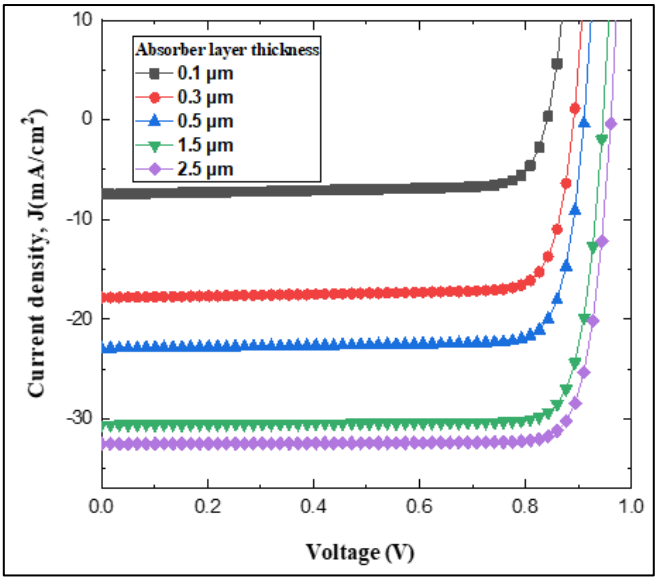

Fig. 3. J-V characteristics of the varying absorber layer thickness.

3.2. Variation of Absorber Layer Thickness

The efficiency, fill factor, JSC, and VOC at each specified value were calculated using a regression analysis model after the models were simulated at varied absorber layer thicknesses. Fig. 4 shows that when the thickness of the absorber layer grows, the fill factor, current density, and open voltage of this configuration all increase [24]. When the absorber layer thickness 0.1 µm, values are the efficiency 4.85%, VOC 0.84V, JSC 7.47 mA/cm2, FF 77.22%. When absorber layer thickness 2.1 µm, values are the efficiency 26.14%, VOC 0.95V, JSC 31.97 mA/cm2, FF 85.53%. At thicker absorber layers, it is hypothesized that the photo-generated electrons and holes will be greatly increased, enhancing the solar cell's overall performance.

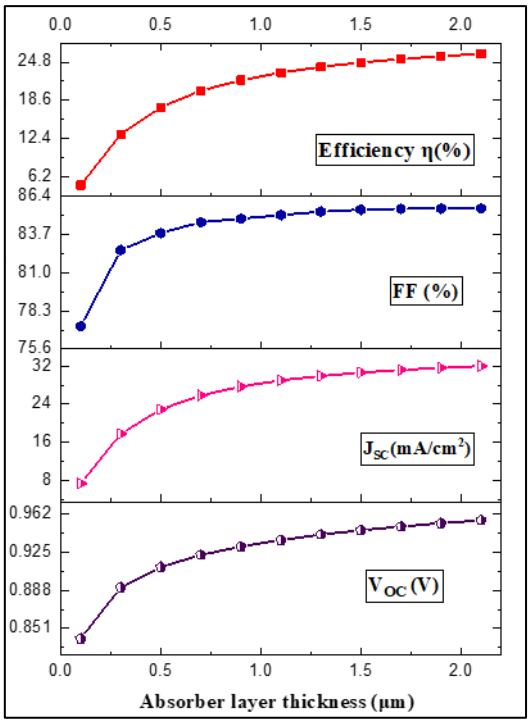

Fig. 4. Absorber Layer Thickness variation of $CsSnGeI_3$ solar cell.

3.3. Effect of Defect Density on Absorber Layer ($CsSnGeI_3$)

Fig. 5 illustrates the relationship between the recommended PSC response to increasing defect densities in the absorber layer as determined by the required perovskite solar cell VOC, JSC, FF, and Efficiency values.

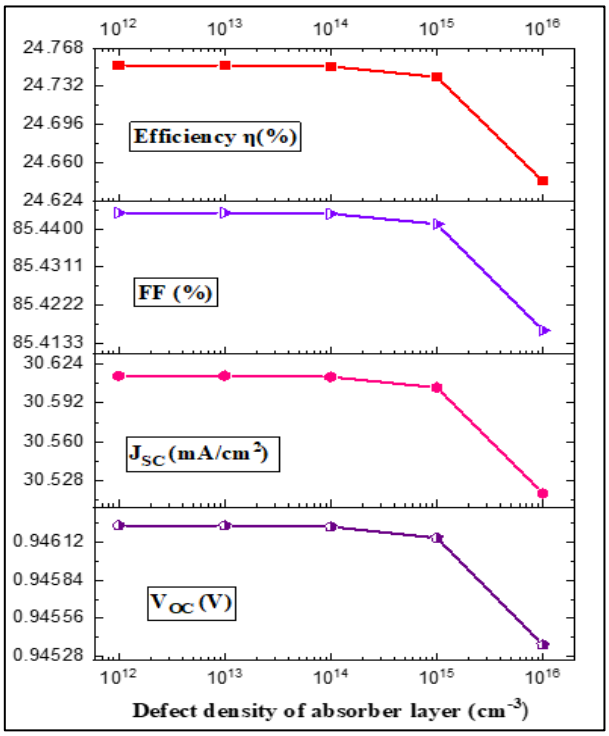

Fig. 5. Impact of the defect density on absorber layer

Defect density of absorber layer's varied from 1012 to 1016 cm-3. The VOC decreased from 0.946 to 0.945 V, JSC 34.61 to 30.51 mA/cm2, FF 85.44 to 85.41%, and Efficiency 24.75 to 24.65% when defect density varied from 1014 to 1016 cm−3Higher defect concentrations in the absorber layer have

the side consequences of larger pinhole generation and recombination due to greater film degradation, poorer stability, and decreased device performance [25]. It has been concluded that an increase in defects causes the diffusion length of the charge carriers to decrease and the number of recombination carriers to rise in the absorber layer, both of which have an immediate effect on efficiency [26].

3.4. Effect of buffer layer thickness on PSC

The behavior of the suggested solar cell is also studied based on varying buffer thickness. By adjusting the buffer layer thickness, Fig. 6 shows the solar cell's output parameters. The buffer layer thickness varied from 0.01 to 0.19 µm. The VOC is obtained to be 0.946 to 0.946 V, JSC 30.41 to 30.04 mA/cm^2, FF 84.94 to 85.50%, and Efficiency 24.85 to 24.75% when buffer layer thickness varying 0.01 to 0.19 µm. The analysis shows the output parameters are stable when varying the buffer thickness. It is because of fewer photons will reach the absorber through the thicker buffer layer, leading to a negligible current for insufficiently produced photo-generated electrons and holes. Therefore, it is projected that a thin buffer layer will produce excellent solar cell performances. The ideal buffer layer thickness has been evaluated to be between 0.05 and 0.06 µm, which is comparable with the buffer thickness used in other studies [27-31]. In this research work, the buffer layer thickness is selected to be 0.05 µm, which is good for improving the PV performance and stability.

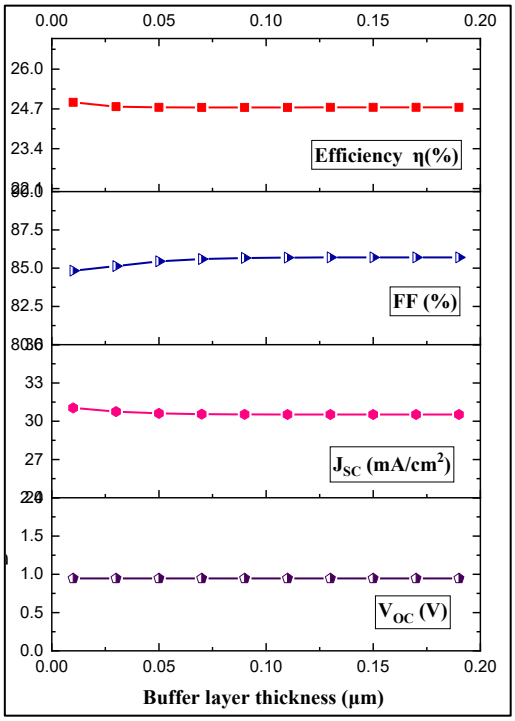

Fig. 6. Impact of the buffer layer thickness

3.5. Effect of temperature on PSC

As with prior recharging studies, operating temperature significantly affects how well solar cell functions [32]. The total performance of the solar cell is impacted by temperature changes. Fig. 7 illustrates how temperature affects efficiency. 300K is the ideal simulation temperature. As shown in the figure for both configurations, the working temperature was then varied between 270K and 450K to assess its effects on PCE, VOC, JSC, and FF for the ideal absorber thickness. When the temperature at 270K, values are efficiency 25.74%, VOC 0.99V, JSC 30.68 mA/cm2, FF 84.55%. When the temperature at 450K, values are efficiency 16.58%, VOC 0.69V, JSC 30.30 mA/cm2, FF 78.28%. It observed that by increasing working temperature efficiency was decreasing. The velocity of charged particles increases as temperature rises [33]. The rate of electron and hole recombination rises as temperature rises because there are fewer free electrons and holes available [34].

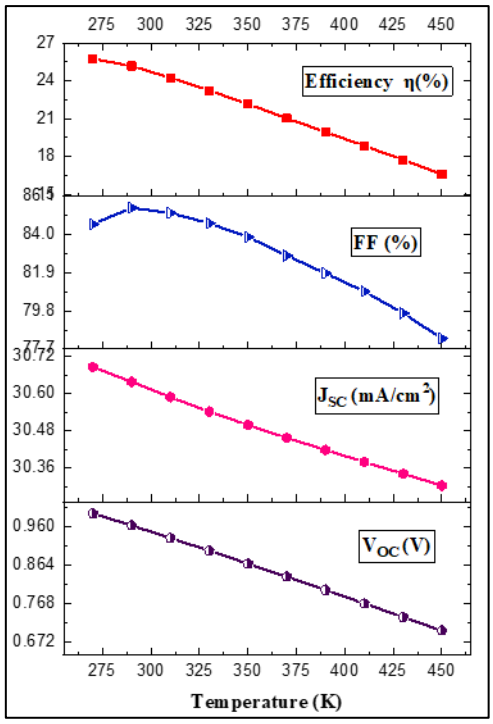

Fig. 7. Impact of the operating temperature.

3.6. Effect of back-contact work function on PSC

As shown in Fig. 8, a material with an appropriate work function at the recommended cell's back-contact characteristics is studied in order to provide a moderate built-in potential there. The range of the back-contact work function was 4.4 to 5.4 eV. Fig. 8 shows that VOC, FF, JSC, and Efficiency rise as the work function is raised. The VOC is increased by 0.143 to 0.966 V, JSC 33.455 to 34.728 mA/cm^2, FF 54.55 to 84.89%, and Efficiency 2.61 to 28.48%. The performance of solar cells is observed to be significantly impacted by the back-contact work function. According to the current modeling findings, a work function greater than 5.1 eV is required for adequate PV performance. Because of its reasonable cost and significant work function, nickel (Ni = 5.35 eV) has been utilized as the back contact in this numerical study to achieve the high performance of a $CsSnGeI_3$-based solar cell [35].

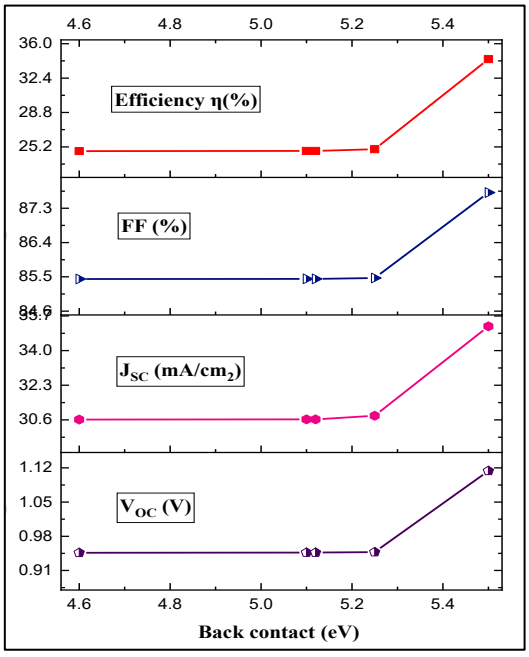

Fig. 8. Impact of the back-contact work function.

3.7. Effect of Series (RS) and Shunt (RSH) Resistances on PSC

The performance of PSC structures is significantly influenced by series (R_S) and shunt (RSH) resistances. These resistances add up to the RS resistance, which connects numerous terminals on the cell's front and rear contacts. The reverse saturation current (RSH), which is brought on by manufacturing flaws, is produced by the active junction. Using the SCAPS-1D simulator, the impact of RS and RSH on solar cell performance such as VOC, JSC, FF, and Efficiency has been assessed as a function of R_S as shown in Fig. 9. The performance is examined by changing R_S between 0 to 5 Ω-cm^2 while RSH is constant at 10^5 Ω-cm^2. Fig. 9 demonstrates that when the R_S increased, the Efficiency and FF dramatically dropped. When R_S was increased from 0 to 5 Ω-cm^2, the Efficiency dropped from 24 to 20% and the FF from 85.60 to 70.09%. These results obtained in this simulation are consistent with the findings reported in previous studies [36,37]. At the same time, JSC and VOC are almost constant, as shown in Fig. 9. JSC and VOC stay stable while RS varied from 0 to 5 Ω-cm^2.

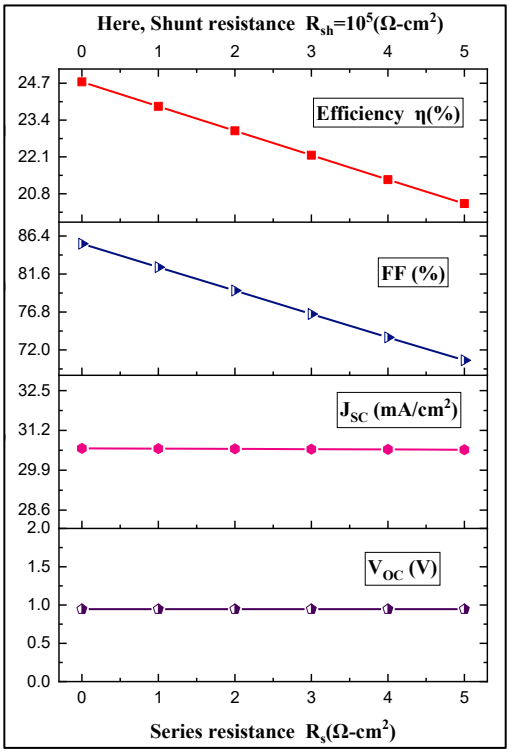

Fig. 9. Impact of the series resistance

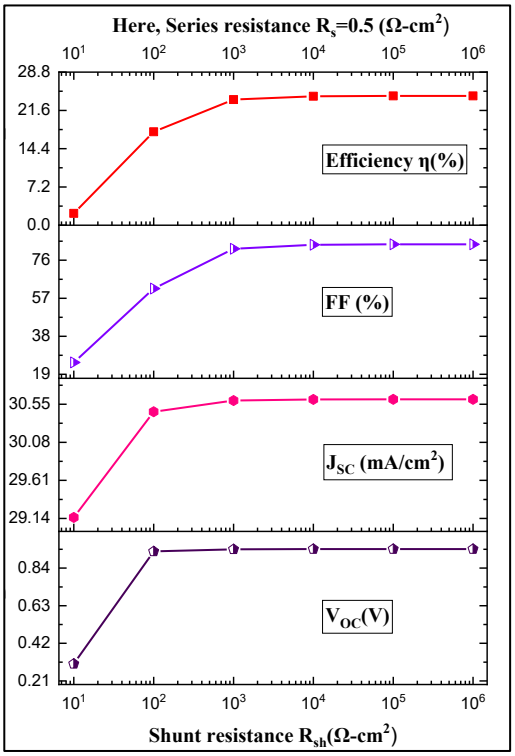

Fig. 10. Impact of the shunt resistance

The suggested perovskite solar cell's output parameters are shown in Fig. 10 as a function of RSH. The impact of RSH is investigated when R_S is held constant at 0.5 Ω-cm^2 and RSH is adjusted from 10^1 to 10^6 Ω-cm^2. Along with the increase in RSH, the VOC rises from 0.304 to 0.946 V, JSC from 29.15 to 30.61 mA/cm^2, FF from 24.01 to 83.95%, and Efficiency from 2.21 to 24.32%. This study has shown that both resistances have a significant impact on the photovoltaic performance of the solar cell.

4. CONCLUSION

The suggested $CsSnGeI_3$ based perovskite thin film solar cell structure is optimized for thickness, device temperature, Resistance effect and defect density in terms of J-V, PCE, FF, Q-E, VOC among other performance characteristics. With a structure of $Al/FTO/TiO_2/CsSnGeI_3/Mo$ and the use of FTO as an ETL, this work develops lead-free $CsSnGeI_3$-based perovskite solar cell. The development of an environmentally friendly perovskite solar cell using a cesium tin-germanium triiodide is demonstrated by these studies. By using SCAPS-1D simulation tools, the effect of changing the absorber layer's thickness is evaluated, and the optimal efficiency is also determined. At a working temperature of 300K, the best result of PCE (24.75%) and an open-circuit voltage of 0.95 V, short-circuit current density of 30.61 mA/cm^2 and a fill factor (FF) of 85.42% was attained at 1.6 μm of absorber layer thickness. Research further shows that the output performance of the suggested device

structure can be enhanced by using suitable back contact materials with a high work function. Mo is used here due to its low price. There are also a few restrictions to take into account while using SCAPS 1D (Solar Cell Capacitance Simulator 1D) to simulate $CsSnGeI_3$-based solar cells. The researchers and scientists will be able to construct the lead-free thin-film solar cell on an experimental scale thanks to this significant increase in efficiency for the practical use of photovoltaic power generation, Building-integrated photovoltaics (BIPV) and Wearable electronics.

References

[1] P. S. Balakrishnan, M. F. Shabbir, A. Siddiqi and X. Wang, "Current status and future prospects of renewable energy: A case study," *Energy Sources, Part A: Recovery, Utilization, and Environmental Effects*, vol. 42, no. 21, pp. 2698-2703, 2020.

[2] M. A. Halim, S. K. Biswas, M. S. Islam and M. M. Ahmed, "Numerical Simulation of Non-toxic ZnSe Buffer Layer to Enhance Sb2S3 Solar Cell Efficiency Using SCAPS-1D Software," *International Journal of Robotics and Control Systems*, vol. 2. no. 4, pp. 709-720, 2022.

[3] M. A. Halim, M. M. Hossain and M. J. Nahar, "Development of a Nonlinear Harvesting Mechanism from Wide Band Vibrations," *International Journal of Robotics and Control Systems*, vol. 2, no. 3, pp. 467-476, 2022.

[4] M. S. J. Marshall, J. Wang, S. Miller, B. Singh and V. Nagarkar, "Developing Perovskite Halide Scintillator thin films for Fast-Timing applications," *2020 IEEE Nuclear Science Symposium and Medical Imaging Conference (NSS/MIC)*, Boston, MA, USA, 2020, pp. 1-2, doi: 10.1109/NSS/MIC42677.2020.9508006.

[5] T. Abzieher *et al*., "Efficient All-Evaporated pin-Perovskite Solar Cells: A Promising Approach Toward Industrial Large-Scale Fabrication," in *IEEE Journal of Photovoltaics*, vol. 9, no. 5, pp. 1249-1257, Sept. 2019, doi: 10.1109/JPHOTOV.2019.2920727.

[6] A. Panda, K. Palodhi, R. Chakraborty and S. Maiti, "Modified thin film perovskite solar cell for high conversion efficiency," *Optik*, vol. 246, p. 167838, 2021.

[7] K. Sobayel *et al*., "A comprehensive defect study of tungsten disulfide (WS2) as electron transport layer in perovskite solar cells by numerical simulation," *Results in Physics*, vol. 12, pp. 1097-1103, 2019.

[8] S. Pescetelli, A. Agresti, S. Razza, L. A. Castriotta and A. Di Carlo, "Large area perovskite solar modules with improved efficiency and stability," *2019 International Symposium on Advanced Electrical and Communication Technologies (ISAECT)*, Rome, Italy, 2019, pp. 1-5, doi: 10.1109/ISAECT47714.2019.9069679.

[9] H. Sabbah, "Numerical simulation of 30% efficient lead-free perovskite CsSnGeI3-based solar cells," *Materials*, vol. 15, no. 9, p. 3229, 2022.

[10] M. S. Rahman, S. Miah, M. S. W. Marma and M. Ibrahim, "Numerical Simulation of CsSnI3-based Perovskite Solar Cells: Influence of doped-ITO Front Contact," *2020 IEEE REGION 10 CONFERENCE (TENCON)*, Osaka, Japan, 2020, pp. 140-145, doi: 10.1109/TENCON50793.2020.9293828.

[11] M. -E. Yeoh and K. -Y. Chan, "A Review on Semitransparent Solar Cells for Real-Life Applications Based on Dye-Sensitized Technology," in *IEEE Journal of Photovoltaics*, vol. 11, no. 2, pp. 354-361, March 2021, doi: 10.1109/JPHOTOV.2020.3047199.

[12] W. C. Chen *et al*., "High luminescence and external quantum efficiency in perovskite quantum-dots light-emitting diodes featuring bilateral affinity to silver and short alkyl ligands," *Chemical Engineering Journal*, vol. 414, pp. 128866, 2021.

[13] M. Kari and K. Saghafi, "Current-voltage hysteresis reduction of CH3NH3PbI3 planar perovskite solar cell by multi-layer absorber," *Micro and Nanostructures*, vol. 165, p. 207207, 2022.

[14] K. J. Savill, A. M. Ulatowski and L. M. Herz, "Optoelectronic properties of tin–lead halide perovskites," *ACS Energy Letters*, vol. 6, no. 7, pp. 2413-2426, 2021.

[15] S. H. Zyoud, A. H. Zyoud, N. M. Ahmed and A. F. Abdelkader, "Numerical modelling analysis for carrier concentration level optimization of CdTe heterojunction thin film–based solar cell with different non–toxic metal chalcogenide buffer layers replacements: using SCAPS–1D software," *Crystals*, vol. , no. 12, p. 1454, 2021.

[16] R. Raghvendra, R. Kumar and S. K. Pandey, "Performance evaluation and material parameter perspective of eco-friendly highly efficient CsSnGeI3 perovskite solar cell," *Superlattices Microstruct.*, vol. 135, p. 106273, 2019.

[17] J. Gulomov, O. Accouche, R. Aliev, B. Neji, R. Ghandour, I. Gulomova and M. Azab, "Geometric optimization of perovskite solar cells with metal oxide charge transport layers," *Nanomaterials*, vol. 12, no. 15, p. 2692, 2022.

[18] S. S. Hussain *et al*., "Numerical modeling and optimization of lead-free hybrid double perovskite solar cell by using SCAPS-1D," *Journal of Renewable Energy*, vol. 2021, pp. 1-12, 2021.

[19] A. Sunny, S. Rahman, M. M. Khatun and S. R. A. Ahmed, "Numerical study of high performance HTL-free CH3NH3SnI3-based perovskite solar cell by SCAPS-1D," *AIP Advances*, vol. 11, no. 6, p. 065102, 2021.

[20] S. Abdelaziz, A. Zekry, A. Shaker, M. Abouelatta, "Investigating the performance of formamidinium tin-based perovskite solar cell by SCAPS device simulation," *Optical Materials*, vol. 101, p. 109738, 2020.

[21] P. Tiwari *et al*., "Design and Simulation of Efficient SnS-Based Solar Cell Using Spiro-OMeTAD as Hole Transport Layer," *Nanomaterials*, vol. 12, no. 14, p. 2506, 2022.

[22] S. Debnath and M. S. Islam, "Performance Analysis of Perovskite Solar Cell with Inorganic Hole Transport Material using SCAPS-1D," *2022 4th International Conference on Electrical, Computer & Telecommunication Engineering (ICECTE)*, Rajshahi, Bangladesh, 2022, pp. 1-4, doi: 10.1109/ICECTE57896.2022.10114547.

[23] R. A. Rassol, R. F. Hasan and S. M. Ahmed, "Numerical Analysis of SnO2/Zn2SnO4/n-CdS/p-CdTe Solar Cell Using the SCAPS-1D Simulation Software," *Iraqi Journal of Science*, pp. 505-516, 2021.

[24] O. Bajjou, M. Al-Hattab, A. Najim, L. Moulaoui, A. Bakour and K. Rahmani, "Modeling and simulation of a solar cell based on CIGS/CdS/ZnO," *2022 2nd International Conference on Innovative Research in Applied Science, Engineering and Technology (IRASET)*, Meknes, Morocco, 2022, pp. 1-5, doi: 10.1109/IRASET52964.2022.9737875.

[25] S. Rai, B. K. Pandey, D. K. Dwivedi, "Modeling of highly efficient and low cost CH3NH3Pb(I1-xClx)3 based perovskite solar cell by numerical simulation," *Optical Materials*, vol. 100, p. 109631. 2020.

[26] L. Et-taya, T. Ouslimane, A. Benami, "Numerical analysis of earth-abundant Cu2ZnSn(SxSe1-x)4 solar cells based on Spectroscopic Ellipsometry results by using SCAPS-1D," *Solar Energy*, vol. 201, pp. 827-835, 2020.

[27] P. Yan, S. Hu, H. Li, W. Gu and C. Sheng, "Efficient Solar Cell Based on Semitransparent Film of Two-Dimensional Alternating Cation Perovskite," in *IEEE Journal of Photovoltaics*, vol. 13, no. 1, pp. 70-76, Jan. 2023, doi: 10.1109/JPHOTOV.2022.3223235.

[28] A. M. Shaheen, A. R. Ginidi, R. A. El-Sehiemy and S. S. M. Ghoneim, "A Forensic-Based Investigation Algorithm for Parameter Extraction of Solar Cell Models," in *IEEE Access*, vol. 9, pp. 1-20, 2021, doi: 10.1109/ACCESS.2020.3046536.

[29] H. C. Sio *et al*., "3-D Modeling of Multicrystalline Silicon Materials and Solar Cells," in *IEEE Journal of Photovoltaics*, vol. 9, no. 4, pp. 965-973, July 2019, doi: 10.1109/JPHOTOV.2019.2914874.

[30] P. Kumari, B. S. Sengar and A. Kumar, "SCAPS Modelling of solar cells: Deploying a back surface field SnS layer for performance upgradation," *2020 5th IEEE International Conference on Emerging Electronics (ICEE)*, New Delhi, India, 2020, pp. 1-4, doi: 10.1109/ICEE50728.2020.9777010.

[31] K. K. Maurya am d V. N. Singh, " Enhancing the performance of an Sb2Se3-based solar cell by dual buffer layer," *Sustainability*, vol. 13, no. 21, p. 12320, 2021.

[32] M. Al-Hattab, M. Khenfouch, O. Bajjou, Y. Chrafih and K. Rahmani, "Numerical simulation of a new heterostructure CIGS/GaSe solar cell system using SCAPS-1D software," *solar energy*, vol. 227, pp. 13-22, 2021.

[33] I. Alam and M. A. Ashraf, "Effect of different device parameters on tin-based perovskite solar cell coupled with In2S3 electron transport layer and CuSCN and Spiro-OMeTAD alternative hole transport

layers for high-efficiency performance," *Energy Sources, Part A: Recovery, Utilization, and Environmental Effects*, pp. 1-17, 2020.

[34] D. K. Sharma, S. K. N, M. S. Ilango and S. K. Ramasesha, "Efficiency Enhancement of the CdS/CdTe Solar Nanostructured Cell Using Electron-Reflecting Layer," in *IEEE Transactions on Electron Devices*, vol. 68, no. 3, pp. 1129-1134, March 2021, doi: 10.1109/TED.2021.3051356.

[35] A. M. Rahman, "Enhancing the photovoltaic performance of Cd-free Cu2ZnSnS4 heterojunction solar cells using SnS HTL and TiO2 ETL," *Solar Energy*, vol. 215, pp. 64-76, 2021.

[36] A. Basak and U. P. Singh, "Numerical modelling and analysis of earth abundant Sb2S3 and Sb2Se3 based solar cells using SCAPS-1D," *Solar Energy Materials and Solar Cells*, vol. 230, p. 111184, 2021.

[37] Y. Luo, J. Lai, N. Yan, W. An and K. Ma, "Integration of Aperture-Coupled Multipoint Feed Patch Antenna With Solar Cells Operating at Dual Compressed High-Order Modes," in *IEEE Antennas and Wireless Propagation Letters*, vol. 20, no. 8, pp. 1468-1472, Aug. 2021, doi: 10.1109/LAWP.2021.3087500.

[38] B. K. Ravidas, M. K. Roy and D. P. Samajdar, "Photovoltaic Performance Metrics of CsSnI3 Perovskite Solar Cells using SCAPS-1D," *2022 IEEE 6th Conference on Information and Communication Technology (CICT)*, Gwalior, India, 2022, pp. 1-5, doi: 10.1109/CICT56698.2022.9997957.

[39] M. Abdelfatah, W. Ismail, N. M. El-Shafai A. El-Shaer, "Effect of thickness, bandgap, and carrier concentration on the basic parameters of Cu2O nanostructures photovoltaics: numerical simulation study," *Materials Technology*, vol. 36, no. 12, pp. 712-720, 2021.